

Article

Mineralogical and Geochemical Characteristics of Lithium and Rare Earth Elements in High-Sulfur Coal from the Donggou Mine, Chongqing, Southwestern China

Jianhua Zou ^{1,*} , Longfei Cheng ¹, Yuanchen Guo ¹, Zhengcheng Wang ¹, Heming Tian ² and Tian Li ²

¹ College of Civil Engineering, Chongqing Three Gorges University, Chongqing 404020, China; 20070003@sanxiau.edu.cn (L.C.); 20100008@sanxiau.edu.cn (Y.G.); 20171004@sanxiau.edu.cn (Z.W.)

² Chongqing Key Laboratory of Exogenic Mineralization and Mine Environment, Chongqing Institute of Geology and Mineral Resources, Chongqing 400042, China; heming1986824@126.com (H.T.); lt_litian@163.com (T.L.)

* Correspondence: zoujianhua@sanxiau.edu.cn; Tel.: +86-23-58102281

Received: 3 June 2020; Accepted: 13 July 2020; Published: 15 July 2020



Abstract: Coal and coal by-products are considered as the potential raw materials for critical elements (e.g., rare earth elements, Li, Ga, Ge, etc.), which have attracted much attention in recent years. The purpose of this study is to investigate the mineralogical and geochemical characteristics, and controlling geological factors of lithium and rare earth elements in the Lopingian (Wujiaping Formation) coal from the Donggou Mine, southeastern Chongqing Coalfield, China. Results indicate that lithium and rare earth elements are significantly enriched in the Donggou coals, which could be new potential alternative sources for critical elements. Concentrations of lithium and rare earth elements in the Donggou coals gradually increase from top to bottom. Lithium is mainly associated with kaolinite, while rhabdophane, florencite, goyazite, and xenotime are the main hosts of rare earth elements. The controlling geological factor is the groundwater leaching of underlying tuff, and to a lesser extent, the terrigenous clastic materials input from the top layer of the Kangdian Upland. This study provides mineralization information for lithium and rare earth elements exploration in coal measures.

Keywords: lithium; rare earth elements; enrichment; modes of occurrence; groundwater leaching

1. Introduction

With the development of new energy and energy storage technologies, the consumption of critical elements such as lithium and rare earth elements (REY, or REE if yttrium is excluded) is increasing rapidly [1–5]. In recent years, coal and coal utilization by-products (e.g., coal gangue, coal combustion products, and acid mine drainage) have been considered as alternative sources for these critical elements [6–11].

Anomalies of lithium are uncommon in coals worldwide. High-Li coals have been discovered only in the Krylovsk and Verkhne-Bikinsk coal basins in the Russian Far East [7], Jungar Coalfield [12–14], Ningwu Coalfield [15], and Jincheng Coalfield [16,17] in Northern China. Lin et al. (2018) indicated that the Appalachian bituminous coals have relatively high probabilities of being promising sources of Li in the United States [18]. It is found that Li was evenly distributed in coal fly ash with different particles [19,20] and most of the Li was found to be concentrated in the amorphous glass portion of fly ash from some coal-fired power plants in Shanxi and Inner Mongolia provinces, northern China [20].

Compared with Li, REY in coal has been investigated more intensely. Anomalies of REY in coal and coal by-products were discovered in Russia Far East [21], United Kingdom, Poland [22], Romania [23], China [24–29], and United States [30–33]. Research on extracting REY from coal and coal by-products was recognized by the U.S. Department of Energy (DOE) in 2015 [34]. Taggart et al. (2018) indicated that the combination of HNO₃ leaching and NaOH roasting is a viable method to extract REY in Appalachian and Illinois Basin coal ashes [35]. Wang et al. (2019) showed that 88.15% of REY can be extracted using the method of NaOH-HCl sequential leaching [36].

The southeastern Chongqing Coalfield is one of seven coalfields in Chongqing, southwestern China, which provides basic fuel to the southeastern Chongqing. However, there is a lack of mineralogical and geochemical compositions on coals from this coalfield. In this paper, we report the coal chemistry, mineralogical and geochemical compositions of the Donggou coals, southeastern Chongqing Coalfield, China, with emphasis on the lithium and REY anomalies.

2. Geological Setting

The Donggou mine is located in the southeastern Chongqing Coalfield in Chongqing Municipality, southwestern China (Figure 1). The coal-bearing stratum of the studied area is the Wujiaping Formation (P₃w), which was deposited in the marine facies that is different from the Xuanwei Formation in the continental facies and the Longtan Formation in the marine-continental transitional facies at the same time (Figure 1). The Wujiaping Formation consists of a set of carbonates intercalated with bioclastic rock, chert, and a thin coal seam. It is distributed evenly throughout the southeastern Chongqing Coalfield, and its thickness generally varies from 100 to 200 m (Figure 2A). The lower part is composed of thick layered bioclastic limestone, banded mudstone, a thin layered coal seam (K1 coal seam), and tuff that is distributed in a stable manner in southwestern China and often used as a distinctive coal exploration marker. The K1 coal is the only coal seam of the Wujiaping Formation in the southeastern Chongqing Coalfield, with a thickness of 0.3~3 m. The upper part consists of black-gray mudstone, medium-thick layered limestone, and dark-gray thick layered bioclastic limestone.

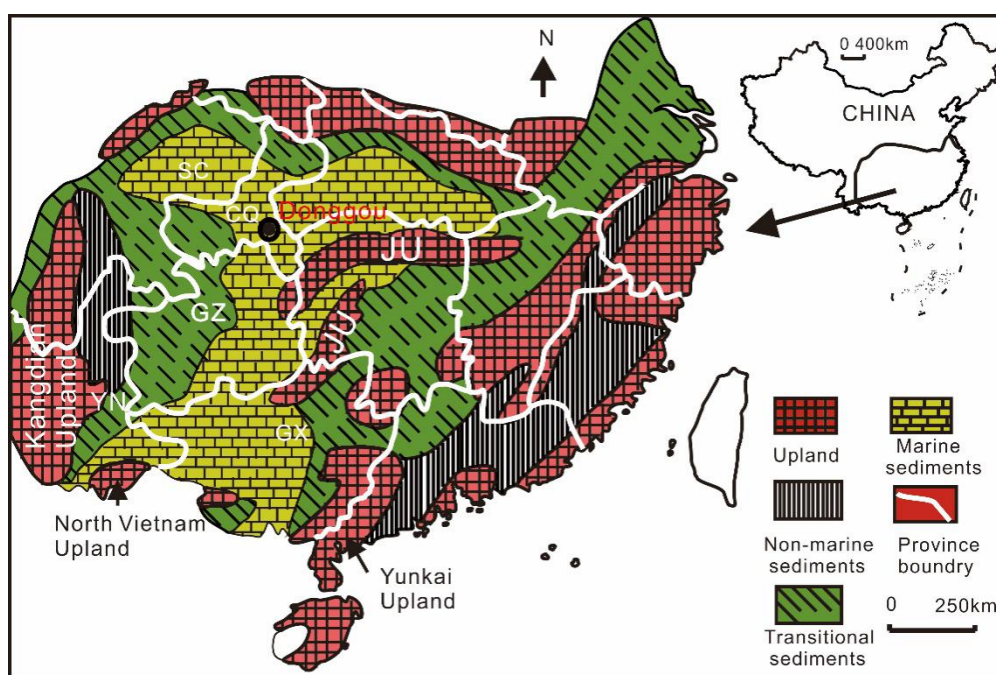


Figure 1. Paleogeography of study area, revised from Dai et al. [37]. JU, Jiangnan Upland; YN, Yunnan Province; GX, Guangxi Province; GZ, Guizhou Province; SC, Sichuan Province; CQ, Chongqing Municipality.

The overlying stratum of the Wujiaping Formation is the Changxing Formation (P_3c), the thickness of which varies from 144 to 173 m. The upper portion is mainly composed of dark gray thick layered bioclastic limestone, with massive or layered chert. The lower part consists of dark gray limestone with siliceous dolomite.

The lowermost stratum of the Wujiaping Formation is the Maokou Formation (P_2m) which is in disconformable contact with the Wujiaping Formation and consists of light, dark gray bioclastic limestone. The upper part is composed of dark grey to grayish black thick layered limestone, mixed with dark grey thin layered siliceous limestone. The lower part includes dark grey to black grey thin-layer marl and thick layered limestone.

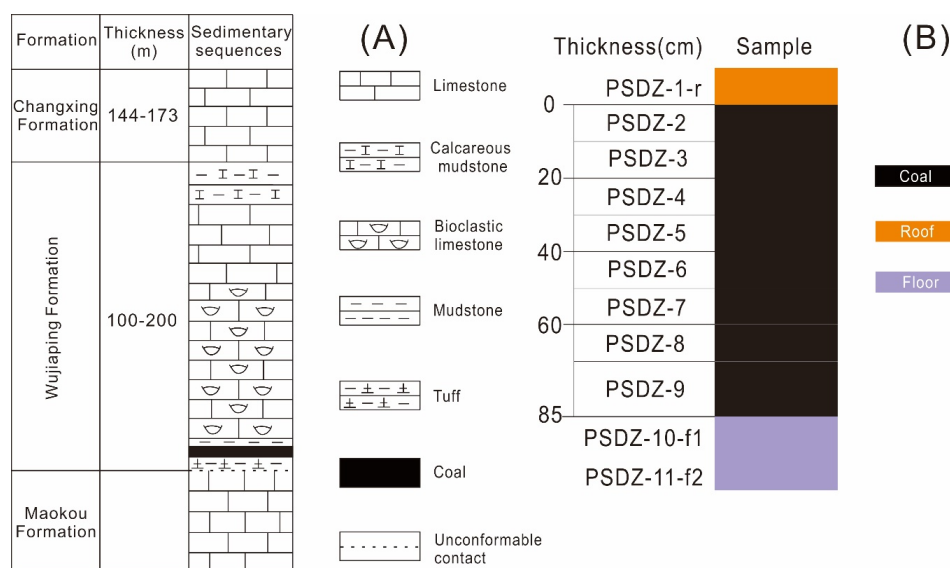


Figure 2. Sedimentary sequences (A), and sampling profile (B) in the Donggou coals.

3. Sampling and Analytical Methods

According to the Chinese standard for coal sampling (GB/T 482-2008) [38], 11 samples were collected from a working surface at the Donggou mine in the southeastern Chongqing Coalfield. These include one roof, two floor (tuff), and eight coal samples. All samples were numbered in an increasing order from top to bottom (Figure 2B). Samples collected in the field were immediately stored in plastic bags to prevent potential contamination and oxidation, and sent to the laboratory for sample preparation.

Polished blocks were prepared for vitrinite random reflectance and scanning electron microscope (SEM) using particles 1 cm. Then all samples were ground to fine powders (<200 mesh) for coal chemistry, mineralogical, and geochemical tests. The proximate analysis (including moisture, ash, and volatile matter) of coal samples was conducted in accordance with ASTM Standards D3173-11 [39], D3174-11 [40], and D3175-11 [41]. The total sulfur was determined using the Eschka method according to ASTM D3177-02 [42] and forms of sulfur in coal were determined according to ASTM D2492-02 [43]. The carbon, hydrogen, and oxygen were measured using an elemental analyzer (VarioMACRO, Elementar, Langensfeld, Germany). The vitrinite random reflectance of coal samples was determined using the Craic QDI 302TM spectrophotometer (Craic Technologies, San Dimas, CA, USA) installed on the Leica DM4500P microscope (Leica Inc., Wetzlar, Germany).

The oxides of major elements were determined by X-ray fluorescence spectrometry (XRF). Prior to XRF analysis, all the samples were ashed at 815 °C. Abundances of trace elements were tested by the inductively coupled plasma mass spectrometry (ICP-MS). Before ICP-MS analysis, the powdered coal and non-coal samples were subjected to microwave digestion using an UltraClave Microwave High Pressure Reactor (Milestone, Sorisole, BG, Italy). The digestion reagents were mixed acid composed of

65% HNO₃ and 40% HF. For coal samples digestion, the volumes of HNO₃ and HF were 5 mL and 2 mL, respectively. For non-coal samples digestion, the volumes of HNO₃ and HF were 2 mL and 5 mL, respectively. HNO₃ and HF were both Guaranteed reagent (GR). The basic loads of the digestion tank consisted of 330 mL ultrapure water, 30 mL H₂O₂, and 2 mL H₂SO₄. Inorganic Ventures standard references (CCS-1, CCS-4, CCS-5, and CCS-6) were used for calibration of trace element concentrations. In order to ensure the stability of ICP-MS, Rh was used as an internal standard.

Coal samples were subjected to low-temperature ashing (LTA) under the condition of <150 °C using the plasma low-temperature ashing instrument (Quorum/Emitech K1050X, Quorum Technologies, Lewes, UK). Then the mineral compositions of coal LTAs and non-coal samples were analyzed by X-ray powder diffraction (XRD). The instrument for the XRD analysis is D/max-2500/PC powder diffractometer (Rigaku Corporation, Tokyo, Japan) with Ni-filtered Cu-K α radiation and a scintillation detector. The XRD pattern was recorded over a 2 θ interval of 2.5~70°, with a step size of 0.02°. After the X-ray diffraction patterns were obtained, the minerals were quantitatively analyzed using Siroquant™ 3.0 software (Siroquant, Mitchell, Australia), which is set out by Rietveld [44] and developed by Taylor [45].

Modes of occurrence of minerals in representative samples were determined by a scanning electron microscope (SEM, JSM-6610LV, JEOL, Tokyo, Japan) equipped with energy-dispersive spectrometer (EDS, OXFORD X-max, Oxford Instruments, Abingdon-on-Thames, UK). Samples were platinum-coated using the JEOL JFC-1600 auto fine coater (JEOL, Tokyo, Japan) prior to SEM-EDS analysis. The analysis conditions of SEM-EDS are: accelerating voltage 20 kV, working distance 10 mm, and high vacuum mode.

4. Results and Discussions

4.1. Coal Chemistry

Table 1 lists data of the proximate and ultimate analysis, forms of sulfur, and vitrinite random reflectance of K1 coal seam in the Donggou Mine, southeastern Chongqing Coalfield. The ash yield of the Donggou coals varies from 15.41% to 43.74% (24.52% on average). Based on the Chinese standard GB/T 15224.1-2010 [46], the Donggou coals are low-medium ash coals. The average values of carbon, hydrogen, and nitrogen are 84.3%, 3.64%, and 1.43%, respectively. Based on Chinese standard GB/T 15224.2-2010 [47], all coals apart from PSDZ-4 are high sulfur coals, with an average of 6.65%. The sulfur in the Donggou coals is mainly pyritic sulfur, followed by organic sulfur and sulfate sulfur. The average values of volatile matter and vitrinite random reflectance are 16.02% and 2.19%, respectively. According to ASTM D388-12 [48], the Donggou coals are classified as low volatile bituminous coal.

Table 1. Proximate and ultimate analysis, forms of sulfur, and vitrinite random reflectance for the Donggou coals (%).

Sample	Proximate Analysis			Ultimate Analysis				Forms of Sulfur			R _{o,ran}
	M _{ad}	A _d	V _{daf}	C _{daf}	H _{daf}	N _{daf}	S _{t,d}	S _{p,d}	S _{s,d}	S _{o,d}	
PSDZ-2	0.69	20.15	12.49	88.22	3.7	1.49	4.47	2.04	0.28	2.15	2.19
PSDZ-3	0.85	18.46	13.24	86.74	3.46	1.53	6.37	2.91	0.48	2.99	2.12
PSDZ-4	0.86	15.41	11.81	89.64	3.74	1.57	2.25	0.74	0.11	1.39	2.23
PSDZ-5	0.76	18.20	12.15	88.97	3.77	1.63	3.04	1.16	0.18	1.71	2.22
PSDZ-6	0.86	20.41	12.63	88.13	3.71	1.53	4.42	1.9	0.33	2.18	2.23
PSDZ-7	0.85	23.62	14.32	86.55	3.67	1.5	5.79	2.65	0.56	2.59	2.19
PSDZ-8	1.38	43.74	26.51	72.96	3.57	1.08	12.56	6.75	1.25	4.56	2.21
PSDZ-9	1.42	36.15	25.01	73.18	3.47	1.11	14.28	7.21	2.12	4.95	2.16
Average	0.96	24.52	16.02	84.30	3.64	1.43	6.65	3.17	0.66	2.82	2.19

M, moisture; A, ash yield; V, volatile matter; C, carbon; H, hydrogen; N, nitrogen; S_t, total sulfur; S_p, pyritic sulfur; S_s, sulfate sulfur; S_o, organic sulfur; ad, air-dried basis; d, dry basis; daf, dry and ash-free basis; R_{o,ran}, vitrinite random reflectance.

4.2. Mineralogical Compositions

The low temperature ash yields (LTAs) of coal samples correlated significantly positively with the high temperature ash yields (HTAs) ($R^2 = 0.99$, Figure 3). However, the LTAs are slightly higher than the HTAs, especially sample PSDZ-8 and PSDZ-9, with LTAs of more than 50%, because minerals could be decomposed under high temperature conditions and new minerals could be formed under low temperature environments [49]. The quantitative mineralogical compositions of the Donggou coal LTAs and non-coal samples are presented in Table 2. The dominant minerals of the Donggou coal LTAs are clay minerals (including illite, kaolinite, illite/smectite mixed layer (I/S), and trace amounts of chamosite), and pyrite, followed by jarosite, quartz, and orthoclase. The minerals in the roof are mainly pyrite, clay minerals (including I/S and kaolinite), and quartz, with small amounts of aluminum hydroxide minerals (gibbsite and diaspore) and gypsum. The main minerals in the floor (tuff) are clay minerals (including kaolinite, illite, and a small portion of chlorite and chamosite) and pyrite, followed by anatase and gypsum. In addition to the minerals mentioned above, other trace minerals such as rhabdophane, florencite, goyazite, xenotime, and zircon are also identified under SEM-EDS observation.

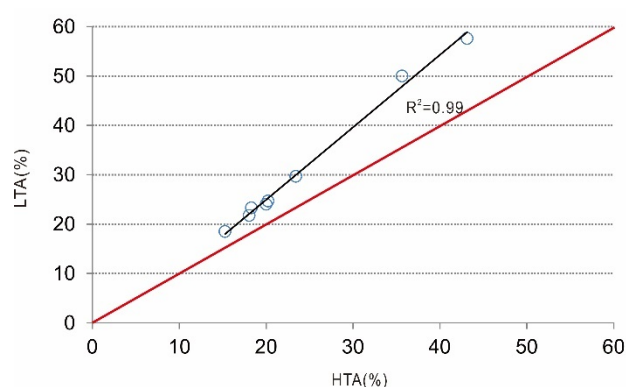


Figure 3. Low temperature ash (LTA) yields versus high temperature ash (HTA) yields of the Donggou coal samples. The red diagonal line in the plot indicates equality.

Table 2. Mineralogical compositions of coal LTAs and non-coal samples in the Donggou mine by XRD and Siroquant analysis (wt. %).

Sample	LTA/HTA*	K	I	I/S	Or	Cha	Chl	Sid	Py	An	Q	Gy	Jar	Gi	Dia
PSDZ-1-r	66.2 *	8.8		29.6					35.2		18	2.2		3.4	2.8
PSDZ-2	24	9.9	42.4		5.1				27.9		13.1		1.7		
PSDZ-3	23.3	7.2	44						43.7		3.2		1.8		
PSDZ-4	18.5	10	40.7	33.1					13.7				2.6		
PSDZ-5	21.7	11.1	49.4	15.1					19.7				4.6		
PSDZ-6	24.7	7.1	41.4	21.3					27.1				3.1		
PSDZ-7	29.6	4.5	37.7	20.8		0.9			33.9				2.2		
PSDZ-8	57.6	28.4	29.3	3.2		1.3			37.8						
PSDZ-9	50	15.5	11.3	8.2					65						
PSDZ-10-f1	76 *	47	37.9			0.8			9.3	4.1		0.9			
PSDZ-11-f2	73.9 *	47.7		25.9			4.5	8.4	4.5	4.8		2.1	2.1		

LTA, low temperature ash yield; HTA, high temperature ash yield; *, HTA; K, kaolinite; I, illite; I/S, illite/smectite mixed layer; Or, orthoclase; Cha, chamosite; Chl, chlorite; Sid, siderite; Py, pyrite; An, anatase; Q, quartz; Gy, gypsum; Jar, jarosite; Gi, gibbsite; Dia, diaspore.

4.3. Elemental Concentrations

Table 3 shows the data of major and trace elements in the Donggou coals. Taking the Chinese common coals as comparative standard [24], concentrations of Fe_2O_3 (7.11%) and K_2O (0.68%) in the Donggou coals are relatively higher. By contrast, concentrations of MnO (0.002%), CaO (0.012%), Na_2O (0.02%), and P_2O_5 (0.013%) are lower than the Chinese common coals [24]. The remaining major elements and ratios of $\text{SiO}_2/\text{Al}_2\text{O}_3$ are close to the Chinese common coals [24].

Dai et al. (2015) proposed an index of concentration coefficient (CC) to characterize the concentration levels of trace elements in coal [50]. CC was defined as the ratio of elemental concentration of studying coals versus that of world hard coals [50,51]. Compared with world hard coals [51], lithium is enriched in the Donggou coals, the CC of which is up to 8.04. The Li concentration of the Donggou coals varies from 6.5 $\mu\text{g/g}$ to 244 $\mu\text{g/g}$, with an average of 96.5 $\mu\text{g/g}$, which is significantly higher than the average value of world hard coals (12 $\mu\text{g/g}$) [51]. This value is slightly lower than that in the Haerwusu coals, Inner Mongolia, China (116 $\mu\text{g/g}$) [12], and that in the Jincheng coals, Qinshui Basin of China (132 $\mu\text{g/g}$) [16]. Note that the Li concentrations of two floor samples (tuff) are up to 898 $\mu\text{g/g}$ and 531 $\mu\text{g/g}$. The Li concentration in the Donggou coals gradually increases from top to bottom (Figure 4). The closer to the tuff, the higher the Li concentration in the Donggou coals (Figure 4).

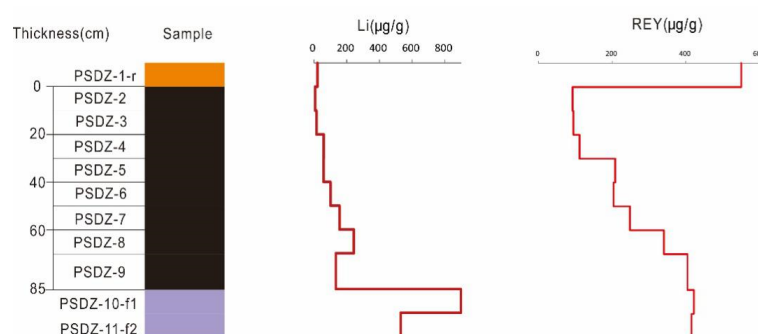


Figure 4. Variations of Li and REY (rare earth elements and yttrium) concentrations along coal seam profiles in the Donggou mine.

The concentration of REY in the Donggou coals is between 92.9 $\mu\text{g/g}$ and 405 $\mu\text{g/g}$, with an average of 213 $\mu\text{g/g}$, higher than the average value of world hard coals (68 $\mu\text{g/g}$) [51]. The average oxides of REY (REO) concentration of the Donggou coal ashes is 1026 $\mu\text{g/g}$, which is higher than the cut-off grade proposed by Seredin and Dai (REO, 1000 $\mu\text{g/g}$ in coal ash) [6]. Similar to the Li distribution in coals, REY concentration also gradually increases from top to bottom of the coal seam (Figure 4).

All the samples do not show distinctive fractionation among light, medium, and heavy REY (Figure 5). Based on the classifications proposed by Seredin and Dai (2012), the REY enrichments in coal are classified as three types: L-type ($\text{La}_N/\text{Lu}_N > 1$), M-type ($\text{La}_N/\text{Sm}_N < 1$, $\text{Gd}_N/\text{Lu}_N > 1$), and H-type ($\text{La}_N/\text{Lu}_N < 1$) [6]. The roof PSDZ-1 exhibits relatively L-type REY enrichment, with weak Eu negative anomaly. The coal bench samples display M-type and H-type REY enrichments, along with weak negative anomalies. The floor sample PSDZ-10-f shows an M-type REY enrichment, with a weak positive Eu anomaly. The lowermost floor sample PSDZ-11-f has a H-type REY enrichment, along with a relatively weak negative Eu anomaly.

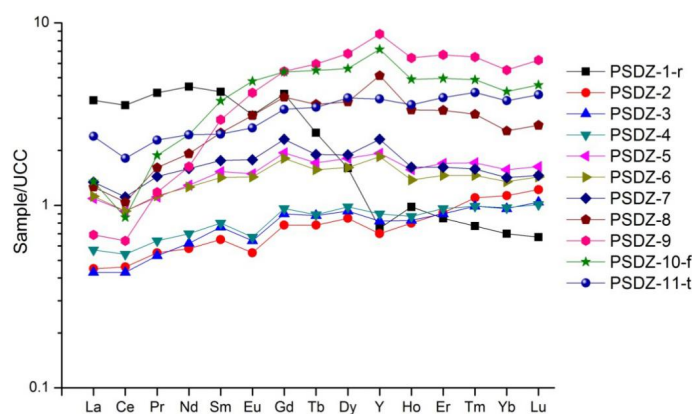


Figure 5. The REY distribution patterns of coal, roof and floor samples in the Donggou mine. The REY data of the upper continental crust (UCC) are cited from Taylor and Mclennan (1985) [52].

Table 3. Major and trace element concentrations of coal and non-coal samples in the Donggou mine ($\mu\text{g/g}$, coal or bulk rock basis).

Sample	PSDZ-1-r	PSDZ-2	PSDZ-3	PSDZ-4	PSDZ-5	PSDZ-6	PSDZ-7	PSDZ-8	PSDZ-9	PSDZ-10-f	PSDZ-11-t	Average	China [24]	World [51]	CC
SiO ₂	29.11	9.21	6.95	7.22	8.09	8.44	8.95	13.96	8.4	34.05	35.77	8.9	8.47		
TiO ₂	0.74	0.44	0.21	0.22	0.36	0.32	0.33	0.5	0.39	2.7	3.21	0.34	0.33		
Al ₂ O ₃	10.96	4.44	4.45	4.94	5.98	6.28	6.97	12.2	7.22	26.79	29.45	6.56	5.98		
Fe ₂ O ₃	20.88	4.12	5.49	1.78	2.62	4.08	5.88	14.72	18.19	6.95	12.68	7.11	4.85		
MnO	0.097	0.002	0.001	0.001	0.001	0.002	0.002	0.005	0.004	0.011	0.062	0.002	0.015		
MgO	0.62	0.22	0.23	0.19	0.16	0.25	0.29	0.31	0.21	1.01	0.63	0.23	0.22		
CaO	0.43	0.14	0.09	0.1	0.12	0.1	0.11	0.17	0.13	0.35	0.45	0.12	1.23		
Na ₂ O	bdl	0.014	0.027	0.027	0.028	0.034	0.032	bdl	bdl	0.021	bdl	0.02	0.16		
K ₂ O	2.36	1.18	0.7	0.62	0.47	0.53	0.59	0.78	0.6	2.08	1.96	0.68	0.19		
P ₂ O ₅	0.099	0.006	0.004	0.005	0.008	0.009	0.011	0.025	0.038	0.096	0.093	0.013	0.092		
SiO ₂ /Al ₂ O ₃	2.66	2.07	1.56	1.46	1.35	1.34	1.28	1.14	1.16	1.27	1.21	1.42	1.42		
Li	21.2	6.5	14.4	59.1	57.8	100	156	244	134	898	531	96.5	31.8	12	8.04
Be	2.78	4.7	4.22	3.75	3.14	5.18	6.52	5.08	5.25	11	6.01	4.73	2.11	1.6	2.96
B	132	111	124	123	113	nd	129	114	88.6	231	221	115	53	52	2.21
F	441	882	279	268	226	287	291	287	204	887	638	340	130	88	3.87
Sc	5.62	7.39	4.39	3.57	2.9	4.63	5.37	5.36	16.6	25.9	17.8	6.28	4.38	3.9	1.61
V	55.7	51	29.6	25.2	18.1	32.1	37.2	105	413	408	548	88.9	35.1	25	3.56
Cr	116	31	23.3	21.1	16.2	37.2	36.7	47.7	397	727	975	76.3	15.4	16	4.77
Co	17.3	2.48	3.48	2.98	3.23	4.36	5	12.1	18.9	15.2	31.1	6.57	7.08	5.1	1.29
Ni	46.7	5.96	4.6	6.62	8.24	10.8	14.2	40.2	55.4	100	159	18.2	13.7	13	1.4
Cu	26.1	14.5	23.4	12.9	13.5	18.4	20.8	31.2	64.7	73.3	124	24.9	17.5	16	1.56
Zn	33.4	19	29.8	32.1	28.2	22.5	23.8	18.4	15.3	41.3	33.3	23.6	41.4	23	1.03
Ga	12.4	9.48	8.02	8.24	10.6	12	16	21	15.3	57.3	50.4	12.6	6.55	5.8	2.17
Ge	3.91	14.6	23	18.6	6.4	4.36	6.21	4.04	2.46	3.02	1.61	9.96	2.78	2.2	4.53
As	62	3.91	9.2	2.69	2.87	3.56	5.9	7.39	10.6	12.7	7.3	5.76	3.79	8.3	0.69
Se	45.7	7.44	15.8	11.1	9.31	11.9	14.7	14.6	15.7	11.9	0.7	12.6	2.47	1.3	9.67
Rb	22.1	12.4	7.58	7.17	5.23	7.46	7.48	7.06	5.83	20.3	14.7	7.52	9.25	14	0.54
Sr	61.2	40.3	28.6	27.7	29	25.1	32	48.2	45.5	89.7	364	34.6	140	110	0.31
Y	16.5	15.3	18	19.8	42.5	40.8	50.5	113	191	158	84.2	61.4	18.2	8.4	7.31
Zr	110	187	86.1	196	418	297	212	186	672	650	597	282	89.5	36	7.83
Nb	28.1	14.7	6.88	18.9	52.7	25.9	22.9	23.8	17.8	61.9	84.1	22.9	9.44	3.7	6.2
Mo	26.2	3.17	3.41	3.03	3.11	2.31	3.06	6.11	10.2	3.97	3.15	4.3	3.08	2.2	1.95
Ag	0.41	0.48	0.29	0.68	1.52	1.02	0.59	0.59	2.65	1.99	2.27	0.98	nd	0.095	10.29
Cd	0.63	0.33	0.48	0.72	1.14	1.28	3.35	1.77	1.9	1.78	2.02	1.37	0.25	0.22	6.23
In	0.14	0.04	0.06	0.07	0.11	0.11	0.12	0.23	0.27	0.37	0.38	0.13	0.05	0.031	4.08
Sn	3.38	2.59	1.41	1.46	2.34	1.93	2.19	4.78	17.6	6.37	8.95	4.29	2.11	1.1	3.9
Sb	0.95	bdl	bdl	bdl	bdl	bdl	0.4	0.95	1.38	1.86	3.65	0.91	0.84	0.92	0.99
Cs	11.8	1.44	0.6	0.05	bdl	bdl	1.68	1.2	bdl	4.12	9.77	0.99	1.13	1	0.99
Ba	42.7	21.3	16.6	13.5	14.1	16.6	17.8	45.2	127	51.9	47	34	159	150	0.23
La	113	13.4	12.9	17.1	32.6	33.7	40.2	37.9	20.6	40.4	71.6	26	22.5	11	2.37
Ce	226	29.4	27.6	34.7	59.5	59.3	71.2	66.5	40.8	55.1	116	48.6	46.7	23	2.11
Pr	29.4	3.9	3.76	4.54	7.85	8.01	10.2	11.5	8.37	13.4	16.2	7.27	6.42	3.5	2.08
Nd	116	15.2	16.1	18.2	33.5	32.7	41.3	50	42.3	63.5	63.4	31.1	22.3	12	2.6
Sm	18.8	2.93	3.43	3.59	6.88	6.4	7.93	11.2	13.3	16.8	11	6.96	4.07	2	3.48
Eu	2.82	0.5	0.57	0.6	1.34	1.29	1.6	2.8	3.73	4.31	2.4	1.55	0.84	0.47	3.31

Table 3. Cont.

Sample	PSDZ-1-r	PSDZ-2	PSDZ-3	PSDZ-4	PSDZ-5	PSDZ-6	PSDZ-7	PSDZ-8	PSDZ-9	PSDZ-10-f	PSDZ-11-t	Average	China [24]	World [51]	CC
Gd	15.5	2.95	3.42	3.64	7.35	6.86	8.73	14.9	20.6	20.5	12.8	8.56	4.65	2.7	3.17
Tb	1.5	0.47	0.53	0.54	1.03	0.94	1.14	2.15	3.57	3.3	2.07	1.3	0.62	0.32	4.05
Dy	5.6	2.99	3.26	3.44	6.33	5.64	6.61	12.9	23.7	19.7	13.6	8.12	3.74	2.1	3.87
Ho	0.78	0.64	0.66	0.7	1.25	1.1	1.3	2.67	5.14	3.92	2.85	1.68	0.96	0.54	3.12
Er	1.95	2.09	2.07	2.2	3.91	3.35	3.72	7.63	15.4	11.4	8.98	5.04	1.79	0.93	5.42
Tm	0.23	0.33	0.3	0.3	0.51	0.44	0.47	0.95	1.95	1.46	1.25	0.66	0.64	0.31	2.11
Yb	1.54	2.49	2.11	2.13	3.45	2.96	3.13	5.64	12.1	9.27	8.25	4.25	2.08	1	4.25
Lu	0.2	0.37	0.31	0.3	0.49	0.43	0.44	0.83	1.88	1.37	1.21	0.63	0.38	0.2	3.15
Hf	3.18	3.91	2.22	4.84	10.7	7.02	5.37	4.86	9.49	15.2	16	6.05	3.71	1.2	5.05
Ta	2.45	0.78	0.53	1.71	2	2.15	1.58	2.08	0.8	4.58	6.07	1.45	0.62	0.28	5.19
W	0.91	0.85	bdl	0.38	1.95	bdl	1	2.5	1.54	2.42	2.98	1.37	1.08	1.1	1.24
Hg	1.04	0.19	0.23	0.2	0.21	0.35	0.46	1.05	1.33	1.48	0.08	0.5	0.16	0.1	5.05
Tl	1.01	0.11	0.07	0.11	0.31	0.42	0.72	0.29	0.19	0.19	0.18	0.28	0.47	0.63	0.44
Pb	64.1	19.6	42.3	11.1	10.7	15.5	32.9	81	89.4	37.6	18.8	37.8	15.1	7.8	4.85
Bi	0.03	0.2	0.19	0.23	0.12	0.37	0.32	0.37	0.28	1.21	1.51	0.26	0.79	0.97	0.27
Th	6.48	5.47	3.42	5.21	5.35	7.61	6.43	11.2	6.21	17.1	21.3	6.35	5.84	3.3	1.93
U	3.16	5.51	1.6	1.47	2.98	9.49	16.3	22.5	30.2	22.1	15.5	11.3	2.43	2.4	4.69

CC [50], concentration coefficient, equals the element concentration in present study versus the respective average element concentration in world hard coals. bdl, below detection limit. nd, no data.

4.4. Modes of Occurrence of Li and REY

Although the modes of occurrence of elements include minerals, organic, and intimate organic associations [53], minerals are generally considered as the major hosts for most elements present in coal [54]. Due to its low atomic number (No.3), lithium cannot be detected by the SEM-EDS. Some studies have shown that Li is mainly present in clay minerals [12,55,56]. There is also an opinion that Li in coal has both organic and inorganic affinities [57]. Finkelman et al. (2018) suggested that Li in most coals is dominantly (90%) associated with clays and micas [58]. Quartz, chalcedony, cristobalite, zircon, and tourmaline are also the hosts of lithium in coal [54]. Zhao (2015) conducted a stepwise chemical extraction method to study the modes of occurrence of Li in coals from the Jungar Coalfield [56]. It was found that Li in coal was bound predominantly to the aluminosilicate minerals [56]. Hu et al. (2018) indicated that lithium in the coal ash was strongly correlated with Al and Si [20]. Cookeite, a Li-bearing chlorite, which is uncommon in coal, was found to be the host of the abundant Li in the No. 15 coal of the Jincheng Coalfield, northern China [16,17]. Dai (2012) identified chlorite phase containing lithium in the Guanbanwusu coals [13].

The correlation coefficient between Li and ash yield in the Donggou coals is 0.74, indicating that Li has an inorganic affinity (Figure 6A). The correlation coefficients of Li-SiO₂ and Li-Al₂O₃ are 0.75 (Figure 6B) and 0.90 (Figure 6C), respectively, further demonstrating that Li mainly occurs as aluminosilicates. As mentioned above, the aluminosilicate minerals in the Donggou coals include kaolinite, illite, and I/S. Moreover, the correlation coefficients of Li-kaolinite (Figure 6D), Li-illite (Figure 6E), and Li-I/S (Figure 6F) are 0.91, 0.13, and 0.10, respectively, indicating that Li in the Donggou coals is mainly associated with kaolinite. The correlation coefficients of Li-sulfur and P₂O₅ are 0.66 and 0.66, respectively, showing that the sulfur and phosphorous-containing minerals may host partial lithium.

Eskenazy (1987) found that REY in Bulgaria coals have an inorganic affinity and are mainly in the form of aluminosilicates [59]. Finkelman et al. (2018) demonstrated that phosphate minerals are the main hosts of REY in bituminous coals, while clay minerals are the dominant hosts of REY in the low-rank coals [58]. However, Seredin (1996) indicated that REY are mainly associated with organic matter, while minerals play an insignificant role in total REY concentration in the Far East, Russia [21]. Arbuzov et al. (2019) concluded that the modes of occurrence of REY in coal change with rank advance [60]. In low rank coals such as brown coals, the dominant hosts of REY are organic matter, while in hard coals or anthracites, the main hosts of REY are authigenic minerals [60]. Zhao et al. (2019) suggested that Light REY in the Jincheng No. 15 coal, northern China, are predominantly associated with phosphate minerals, while heavy REY show a mixed phosphate and organic affinity [16]. Although REY in coals, especially in low-rank coals, have an association with organic matter, it is generally considered that minerals host REY significantly in coal [53]. Compared with LREY, HREY are often more apt to have an organic affinity, probably because the HREY are easier to be captured by organic matter to form organometallic complexes [53].

The correlation coefficient between REY and ash yield in the Donggou coals is 0.84 (Figure 7A), indicating that REY are mainly present in inorganic matter. The correlation coefficients of REY-Al₂O₃, REY-SiO₂ and REY-P₂O₅ are 0.63 (Figure 7B), 0.76 (Figure 7C), and 0.88 (Figure 7D), respectively, indicating that aluminosilicates and phosphorous-containing minerals host REY in the Donggou coals. Under SEM-EDS observation, some REY-bearing phosphate minerals, including rhabdophane (Figure 8A,B), florencite (Figure 8C,D), goyazite (Figure 8E,F), and xenotime (Figure 8G,H) were directly identified, which are the dominant hosts of REY in the Donggou coals.

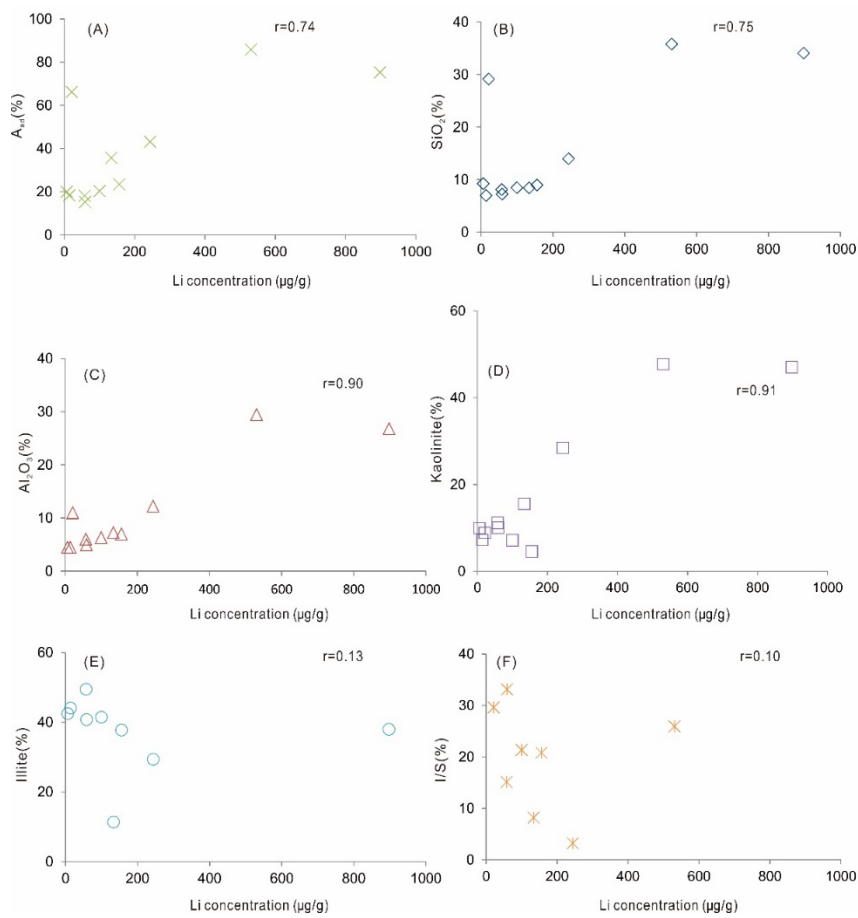


Figure 6. Relations between lithium and ash yield (A_{ad}) (A), SiO_2 (B), Al_2O_3 (C), kaolinite (D), illite (E), and I/S (F) of the Donggou coals. A_{ad} , ash on air dry basis. r, correlation coefficient.

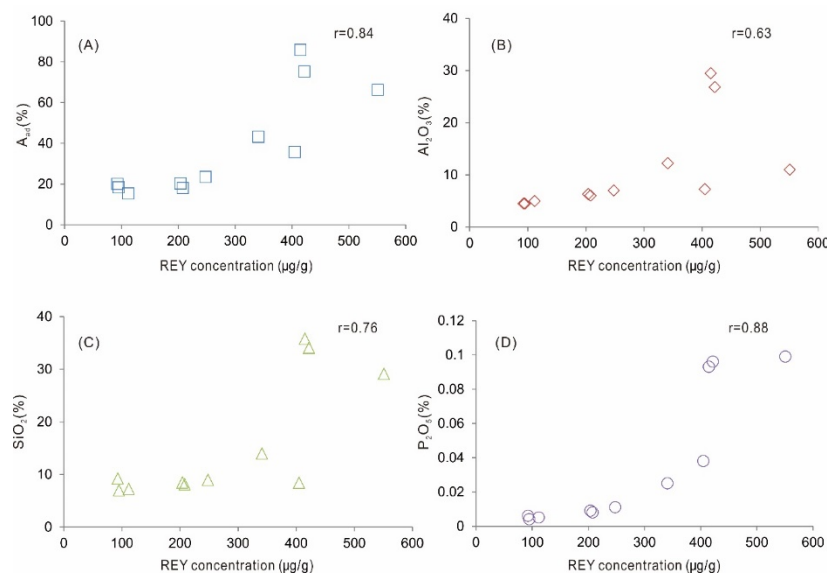


Figure 7. Relations between REY and ash yield (A_{ad}) (A); Al_2O_3 (B), SiO_2 (C), and P_2O_5 (D) of coal seam in the Donggou mine.

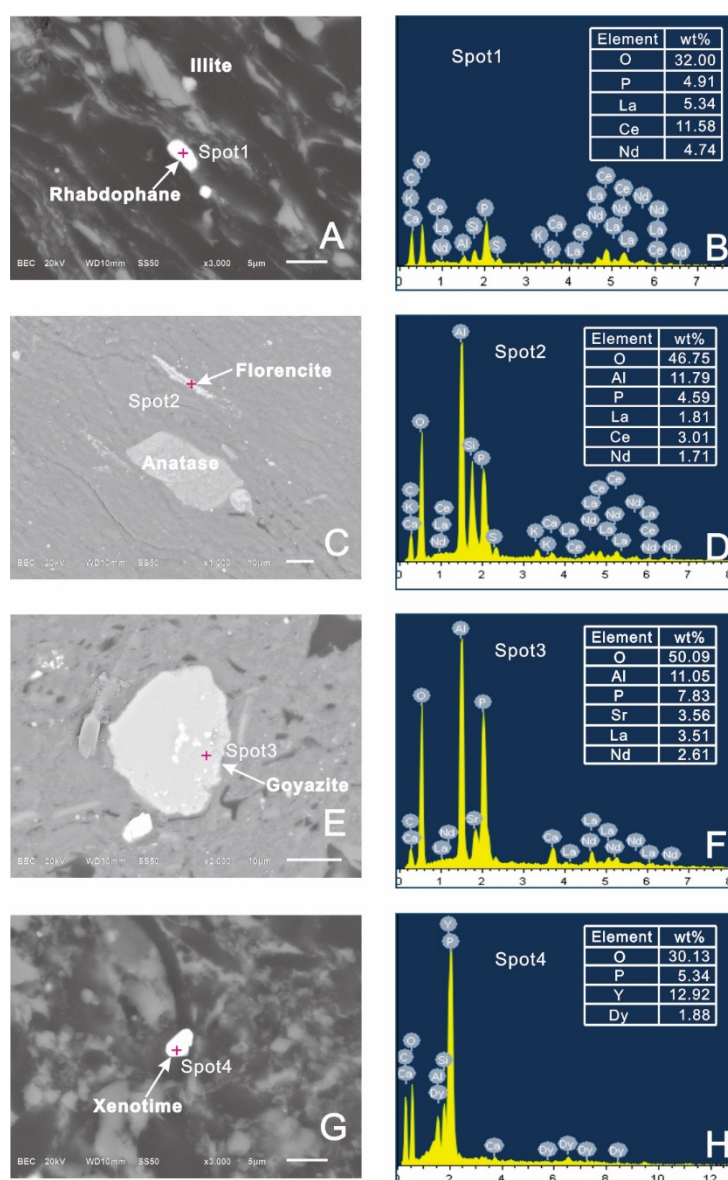


Figure 8. SEM back-scattering images of rhabdophane, florencite, goyazite, and xenotime of samples in the Donggou mine. (A) rhabdophane and illite in sample PSDZ-2. (B) the energy dispersive spectrum data of spot 1. (C) florencite and anatase in sample PSDZ-8. (D) the energy dispersive spectrum data of spot 2. (E) goyazite in sample PSDZ-10-f1. (F) the energy dispersive spectrum data of spot 3. (G) xenotime in sample PSDZ-5. (H) the energy dispersive spectrum data of spot 4.

4.5. Controlling Geological Origin

The enrichment and depletion of trace elements in coal are mainly affected by geological factors such as terrigenous clastic material input, volcanic ash eruption, hydrothermal leaching and sedimentary environment [49,61–63]. To a specific coalfield, there is always one or more geological factors influencing the enrichment and depletion of trace elements in coal. In the present study, the terrigenous materials of the Donggou coals originated from the felsic-intermediate rocks at the top of the Kangdian Upland. Anomalous concentrations of Li and REY in overlying coals are mainly a result of the groundwater leaching from underlying tuff.

4.5.1. Indications of $\text{Al}_2\text{O}_3/\text{TiO}_2$

Owing to the stable nature of Al_2O_3 and TiO_2 , the $\text{Al}_2\text{O}_3/\text{TiO}_2$ ratio in igneous-derived sedimentary materials is usually invariable during the alteration of parent magma [64]. Thus, the $\text{Al}_2\text{O}_3/\text{TiO}_2$ ratio is considered as a reliable index to discriminate the source region in sedimentary rocks including coal [49]. The $\text{Al}_2\text{O}_3/\text{TiO}_2$ ratios, 3–8, 8–21, and 21–70 for sedimentary rocks, imply the source region being mafic, intermediate, and felsic igneous rocks, respectively [64]. The $\text{Al}_2\text{O}_3/\text{TiO}_2$ ratios of roof, floor, and coal samples, except samples PSDZ-4 and PSDZ-8, fall in an area between 8 and 21 (Figure 9), indicating that the sediment source region of the Donggou coals is of intermediate composition. The $\text{Al}_2\text{O}_3/\text{TiO}_2$ ratios of coal samples PSDZ-4 and PSDZ-8 are higher than 21, implying that the sediment source region may have, more or less, felsic compositions. The Kangdian Upland, a well-known sediment source region for most late Permian coals in southwestern China, is composed of tholeiitic and high-Ti basalts with trachytes and/or rhyolites at the top of the sequence. On the basis of the chemical compositions, the terrigenous materials were mainly from the felsic-intermediate rocks at the top of the Kangdian Upland, which is similar to the Dahebian coals [49].

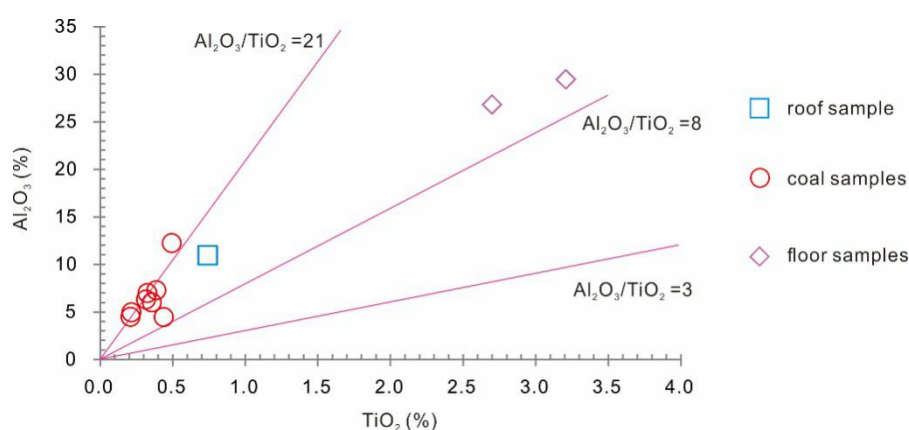


Figure 9. Relationships between Al_2O_3 and TiO_2 of coal seam in the Donggou mine.

4.5.2. Redistribution of Li and REY by Leaching

Lithium and REY concentrations gradually increase from top to bottom (Figure 4). The closer to the tuff (floor of the coal seam), the higher the concentrations of Li and REY in the Donggou coals (Figure 4). The underlying tuff may act as a dominant donor of elements including Li and REY, while the overlying coal operates as a recipient [49]. In addition, the groundwater leaching process may have led to redistribution of some element pairs such as Nb/Ta, Zr/Hf, and U/Th in coal, parting, roof, and floor [65,66]. As the former element is relatively easier to be leached, the ratios of Nb/Ta, Zr/Hf, and U/Th of coal are generally higher than those of the adjacent roof and floor (Figure 10) [65,66]. Therefore, anomalies of Li and REY in the Donggou coals may mainly be a result of the groundwater leaching from underlying tuff, which is similar to the REY redistribution mechanism in the Heidaigou [67] and Dahebian [49] coals.

Moreover, the hypothesis that Li and REY anomalies were subjected by groundwater leaching is supported by modes of occurrence of rhabdophane (Figure 8A), florencite (Figure 8B), goyazite (Figure 8C), xenotime (Figure 8D), and Zircon (Figure 11). These authigenic minerals could be redeposited as secondary minerals in the Donggou coals after the REY and Zr were leached out from the underlying tuff [68].

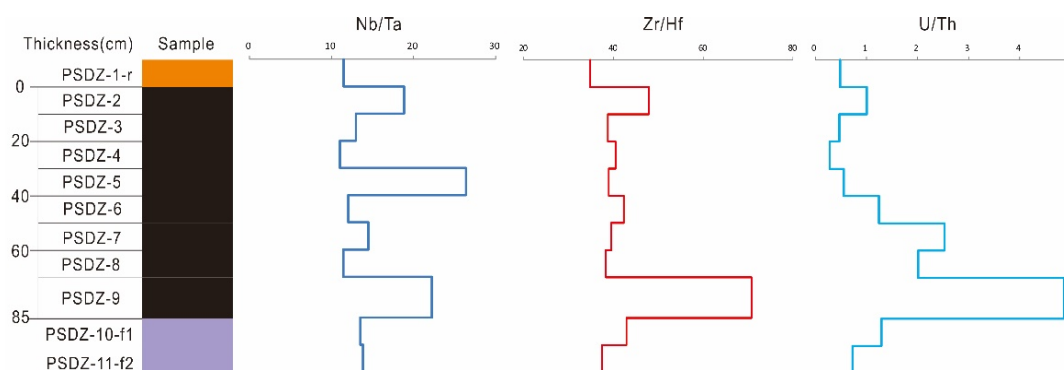


Figure 10. Nb/Ta, Zr/Hf and U/Th ratio variations in coal seam profile from the Dongzhou mine.

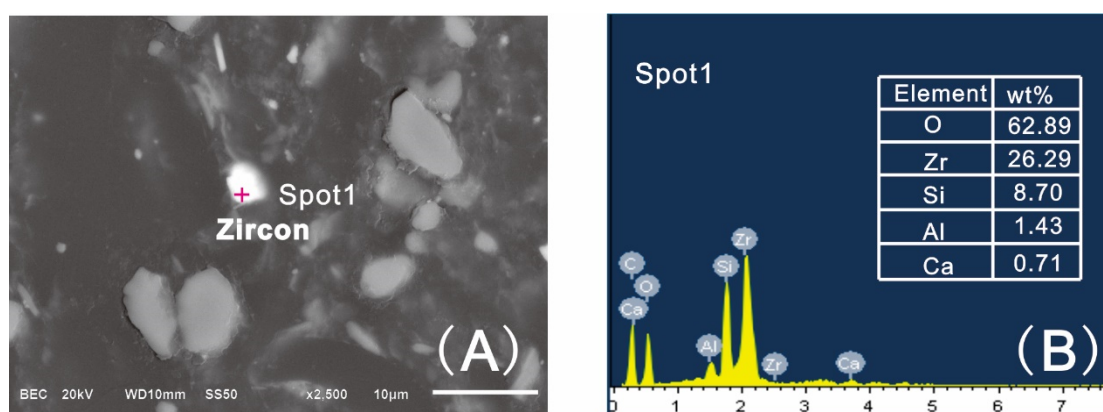


Figure 11. SEM back-scattering images of zircon in sample PSDZ-2 from the Donggou mine (A) and the energy dispersive spectrum data of spot 1 (B).

4.6. Preliminary Economic Evaluation of REY and Li

Seredin and Dai (2012) proposed the cut-off grade of REY in the coal ash (REO in coal ash is 1000 $\mu\text{g/g}$) [6]. In addition, in order to further evaluate the economic significance of REY, a three-fold classification was used based on the REY supply and demand relationships [6]. REY were divided into critical (including Nd, Eu, Tb, Dy, Y, and Er), uncritical (including La, Sm, Pr, and Gd), and excessive (including Ce, Ho, Tm, Yb, and Lu) groups [6,69]. An index called outlook coefficient (C_{outl}) was defined as the ratio of the proportion of critical REY in total REY to the proportion of excessive REY in total REY [6]. The $C_{\text{outl}} > 1$ represents REY in coal ash being highly promising, $0.7 < C_{\text{outl}} < 1.9$ represents it as promising, while $C_{\text{outl}} < 0.7$ is unpromising [70]. According to the classifications based on Dai et al. (2017) [70], a graph of C_{outl} -REY was plotted (Figure 12). It can be seen that there is one coal sample (PSDZ-9) located in the highly promising area, and three coal samples (PSDZ-5, PSDZ-6, and PSDZ-7) located in the promising area. As mentioned above, the average concentration of REY oxides in the Donggou coal ashes is 1026 $\mu\text{g/g}$, higher than the cut-off grade of REY in coal ash [6]. Furthermore, REY types in the Donggou coals are all M-type or H-type enrichments, which have greater economic significance.

Although there is a lack of lithium evaluation criteria like REY in coal, lithium could be co-extracted with REY considering the comprehensive utilization. Thus, the four Donggou coal samples (lower part of K1 coal seam) could be considered as potential alternative sources for extracting REY and Li.

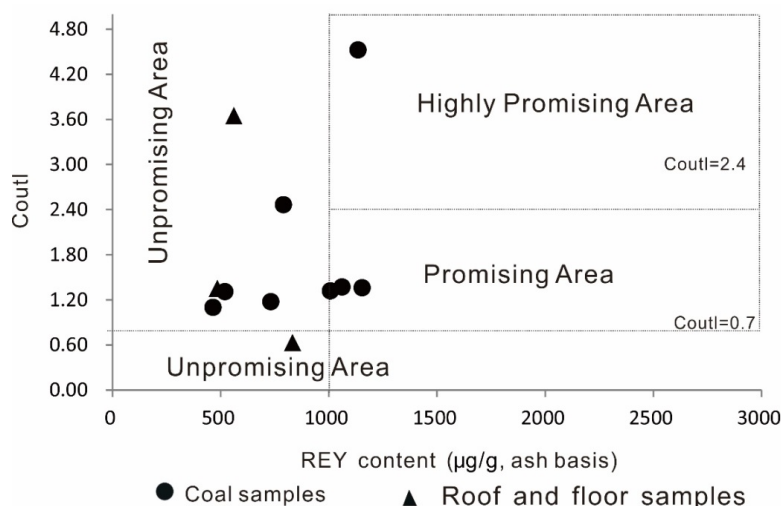


Figure 12. Evaluation of REY in the coal ashes, roof and floor samples in the Donggou mine.

5. Conclusions

The average concentrations of Li and REY in the Donggou coals are 96.5 µg/g and 213 µg/g, which are significantly higher than the average values of world hard coals. Li is mainly associated with kaolinite. REY mainly occurred as rhabdophane, florencite, goyazite, and xenotime. Anomalies of Li and REY in coal are mainly a result of the groundwater leaching from underlying tuff during coalification (either syngenetic, diagenetic or epigenetic), plus a small proportion from the terrigenous materials input from the felsic-intermediate rocks at the top of the Kangdian Upland. The Donggou coal ashes could be considered as potential alternative sources of extracting Li and REY. Coals from the surrounding area that are further enriched in Li and REY might be discovered, which are being studied.

Author Contributions: Conceptualization, J.Z.; methodology, H.T. and T.L.; formal analysis, Z.W.; data curation, J.Z.; writing—original draft preparation, J.Z.; writing—review and editing, J.Z.; funding acquisition, L.C. and Y.G. All authors have read and agreed to the published version of the manuscript.

Funding: This research was funded by the Natural Science Foundation of China, grant number 41502162; the Science and Technology Research Program of Chongqing Municipal Education Commission, grant number KJQN201901230; and the Key Cultivation Project of Chongqing Three Gorges, grant numbers 19ZDPY01 and SXAPGC19YB01.

Acknowledgments: The authors would like to thank Zhen Wang for his assistance in laboratory analysis and Lei Zhao for suggestions on the manuscript preparation. Many thanks are given to academic editors and two anonymous reviewers for their careful and valuable comments, which improve the quality of this manuscript.

Conflicts of Interest: The authors declare no conflict of interest.

References

- Gil-Alana, L.A.; Monge, M. Lithium: Production and estimated consumption. Evidence of persistence. *Resour. Policy* **2019**, *60*, 198–202. [[CrossRef](#)]
- Helbig, C.; Bradshaw, A.M.; Wietschel, L.; Thorenz, A.; Tuma, A. Supply risks associated with lithium-ion battery materials. *J. Clean Prod.* **2018**, *172*, 274–286. [[CrossRef](#)]
- Balaram, V. Rare earth elements: A review of applications, occurrence, exploration, analysis, recycling, and environmental impact. *Geosci. Front.* **2019**, *10*, 1285–1303. [[CrossRef](#)]
- Per, K.; Erika, M. Examining the rare—Earth elements (REE) supply—Demand balance for future global wind power scenarios. *Geol. Surv. Den. Greenl.* **2018**, *41*, 87–90.
- U.S. Geological Survey. *Mineral Commodity Summaries 2019*; U.S. Geological Survey: Reston, VA, USA, 2019.
- Seredin, V.V.; Dai, S. Coal deposits as potential alternative sources for lanthanides and yttrium. *Int. J. Coal Geol.* **2012**, *94*, 67–93. [[CrossRef](#)]
- Seredin, V.V.; Dai, S.; Sun, Y.; Chekryzhov, I.Y. Coal deposits as promising sources of rare metals for alternative power and energy-efficient technologies. *Appl. Geochem.* **2013**, *31*, 1–11. [[CrossRef](#)]

8. Dai, S.; Finkelman, R.B. Coal as a promising source of critical elements: Progress and future prospects. *Int. J. Coal Geol.* **2018**, *186*, 155–164. [[CrossRef](#)]
9. Franus, W.; Wiatros-Motyka, M.M.; Wdowin, M. Coal fly ash as a resource for rare earth elements. *Environ. Sci. Pollut. Res. Int.* **2015**, *22*, 9464–9474. [[CrossRef](#)]
10. Folgueras, M.B.; Alonso, M.; Fernández, F.J. Coal and sewage sludge ashes as sources of rare earth elements. *Fuel* **2017**, *192*, 128–139. [[CrossRef](#)]
11. Qin, S.; Zhao, C.; Li, Y.; Zhang, Y. Review of coal as a promising source of lithium. *Int. J. Oil Gas Coal Technol.* **2015**, *9*, 215. [[CrossRef](#)]
12. Dai, S.; Li, D.; Chou, C.-L.; Zhao, L.; Zhang, Y.; Ren, D.; Ma, Y.; Sun, Y. Mineralogy and geochemistry of boehmite-rich coals: New insights from the Haerwusu Surface Mine, Jungar Coalfield, Inner Mongolia, China. *Int. J. Coal Geol.* **2008**, *74*, 185–202. [[CrossRef](#)]
13. Dai, S.; Jiang, Y.; Ward, C.R.; Gu, L.; Seredin, V.V.; Liu, H.; Zhou, D.; Sun, X.; Zou, J.; Ren, D. Mineralogical and geochemical compositions of the coal in the Guanbanwusu Mine, Inner Mongolia, China: Further evidence for the existence of an Al (Ga and REE) ore deposit in the Jungar Coalfield. *Int. J. Coal Geol.* **2012**, *98*, 10–40. [[CrossRef](#)]
14. Li, J.; Zhuang, X.; Yuan, W.; Liu, B.; Querol, X.; Font, O.; Moreno, N.; Li, J.; Gang, T.; Liang, G. Mineral composition and geochemical characteristics of the Li-Ga-rich coals in the Buertaohai-TianjiaShipan mining district, Jungar Coalfield, Inner Mongolia. *Int. J. Coal Geol.* **2016**, *167*, 157–175. [[CrossRef](#)]
15. Sun, Y.; Zhao, C.; Zhang, J.; Yang, J.; Zhang, Y.; Yuan, Y.; Xu, J.; Duan, D. Concentrations of valuable elements of the coals from the Pingshuo Mining District, Ningwu Coalfield, northern China. *Energ. Explor. Exploit.* **2013**, *31*, 727–744. [[CrossRef](#)]
16. Zhao, L.; Dai, S.; Nechaev, V.P.; Nechaeva, E.V.; Graham, I.T.; French, D. Enrichment origin of critical elements (Li and rare earth elements) and a Mo-U-Se-Re assemblage in Pennsylvanian anthracite from the Jincheng Coalfield, southeastern Qinshui Basin, northern China. *Ore Geol. Rev.* **2019**, *115*, 103184. [[CrossRef](#)]
17. Zhao, L.; Ward, C.R.; French, D.; Graham, I.T.; Dai, S.; Yang, C.; Xie, P.; Zhang, S. Origin of a kaolinite-NH₄-illite-pyrophyllite-chlorite assemblage in a marine-influenced anthracite and associated strata from the Jincheng Coalfield, Qinshui Basin, Northern China. *Int. J. Coal Geol.* **2018**, *185*, 61–78. [[CrossRef](#)]
18. Lin, R.; Soong, Y.; Granite, E.J. Evaluation of trace elements in U.S. coals using the USGS COALQUAL database version 3.0. Part II: Non-REY critical elements. *Int. J. Coal Geol.* **2018**, *192*, 39–50. [[CrossRef](#)]
19. Ma, Z.; Shan, X.; Cheng, F. Distribution Characteristics of Valuable Elements, Al, Li, and Ga, and Rare Earth Elements in Feed Coal, Fly Ash, and Bottom Ash from a 300 MW Circulating Fluidized Bed Boiler. *ACS Omega* **2019**, *4*, 6854–6863. [[CrossRef](#)]
20. Hu, P.; Hou, X.; Zhang, J.; Li, S.; Wu, H.; Damø, A.J.; Li, H.; Wu, Q.; Xi, X. Distribution and occurrence of lithium in high-alumina-coal fly ash. *Int. J. Coal Geol.* **2018**, *189*, 27–34. [[CrossRef](#)]
21. Seredin, V.V. Rare earth element-bearing coals from the Russian Far East deposits. *Int. J. Coal Geol.* **1996**, *30*, 101–129. [[CrossRef](#)]
22. Blissett, R.S.; Smalley, N.; Rowson, N.A. An investigation into six coal fly ashes from the United Kingdom and Poland to evaluate rare earth element content. *Fuel* **2014**, *119*, 236–239. [[CrossRef](#)]
23. Valentim, B.; Abagiu, A.T.; Angheliescu, L.; Flores, D.; French, D.; Gonçalves, P.; Guedes, A.; Popescu, L.G.; Predeanu, G.; Ribeiro, J.; et al. Assessment of bottom ash landfilled at Ceplea Valley (Romania) as a source of rare earth elements. *Int. J. Coal Geol.* **2019**, *201*, 109–126. [[CrossRef](#)]
24. Dai, S.; Ren, D.; Chou, C.-L.; Finkelman, R.B.; Seredin, V.V.; Zhou, Y. Geochemistry of trace elements in Chinese coals: A review of abundances, genetic types, impacts on human health, and industrial utilization. *Int. J. Coal Geol.* **2012**, *94*, 3–21. [[CrossRef](#)]
25. Dai, S.; Nechaev, V.P.; Chekryzhov, I.Y.; Zhao, L.; Vysotskiy, S.V.; Graham, I.; Ward, C.R.; Ignatiev, A.V.; Velivetskaya, T.A.; Zhao, L.; et al. A model for Nb–Zr–REE–Ga enrichment in Lopingian altered alkaline volcanic ashes: Key evidence of H-O isotopes. *Lithos* **2018**, *302*, 359–369. [[CrossRef](#)]
26. Dai, S.; Graham, I.T.; Ward, C.R. A review of anomalous rare earth elements and yttrium in coal. *Int. J. Coal Geol.* **2016**, *159*, 82–95. [[CrossRef](#)]
27. Zhao, L.; Dai, S.; Nechaev, V.P.; Nechaeva, E.V.; Graham, I.T.; French, D.; Sun, J. Enrichment of critical elements (Nb-Ta-Zr-Hf-REE) within coal and host rocks from the Datanhao mine, Daqingshan Coalfield, northern China. *Ore Geol. Rev.* **2019**, *111*, 102951. [[CrossRef](#)]

28. Zou, J.; Liu, D.; Tian, H.; Li, T.; Liu, F.; Tan, L. Anomaly and geochemistry of rare earth elements and yttrium in the late Permian coal from the Moxinpo mine, Chongqing, southwestern China. *Int. J. Coal Sci. Tech.* **2014**, *1*, 23–30. [[CrossRef](#)]
29. Dai, S.; Zhou, Y.; Zhang, M.; Wang, X.; Wang, J.; Song, X.; Jiang, Y.; Luo, Y.; Song, Z.; Yang, Z.; et al. A new type of Nb (Ta)—Zr(Hf)—REE—Ga polymetallic deposit in the late Permian coal-bearing strata, eastern Yunnan, southwestern China: Possible economic significance and genetic implications. *Int. J. Coal Geol.* **2010**, *83*, 55–63. [[CrossRef](#)]
30. Lin, R.; Soong, Y.; Granite, E.J. Evaluation of trace elements in U.S. coals using the USGS COALQUAL database version 3.0. Part I: Rare earth elements and yttrium (REY). *Int. J. Coal Geol.* **2018**, *192*, 1–13. [[CrossRef](#)]
31. Hower, J.; Groppo, J.; Henke, K.; Hood, M.; Eble, C.; Honaker, R.; Zhang, W.; Qian, D. Notes on the Potential for the Concentration of Rare Earth Elements and Yttrium in Coal Combustion Fly Ash. *Minerals* **2015**, *5*, 356–366. [[CrossRef](#)]
32. Hower, J.C.; Eble, C.; Dai, S.; Belkin, H.E. Distribution of rare earth elements in eastern Kentucky coals: Indicators of multiple modes of enrichment? *Int. J. Coal Geol.* **2016**, *160*, 73–81. [[CrossRef](#)]
33. Hower, J.C.; Ruppert, L.F.; Eble, C. Lanthanide, yttrium, and zirconium anomalies in the Fire Clay coal bed, Eastern Kentucky. *Int. J. Coal Geol.* **1999**, *39*, 141–153. [[CrossRef](#)]
34. The U.S. Department of Energy. DOE Selects Projects to Enhance Its Research into Recovery of rare Earth Elements from Coal and Coal Byproducts. Available online: <https://energy.gov/fe/articles/doe-selects-projects-enhance-its-research-recovery-rare-earth-elements-coal-and-coal> (accessed on 5 December 2015).
35. Taggart, R.K.; Hower, J.C.; Hsu-Kim, H. Effects of roasting additives and leaching parameters on the extraction of rare earth elements from coal fly ash. *Int. J. Coal Geol.* **2018**, *196*, 106–114. [[CrossRef](#)]
36. Wang, Z.; Dai, S.; Zou, J.; French, D.; Graham, I.T. Rare earth elements and yttrium in coal ash from the Luzhou power plant in Sichuan, Southwest China: Concentration, characterization and optimized extraction. *Int. J. Coal Geol.* **2019**, *203*, 1–14. [[CrossRef](#)]
37. Dai, S.; Ren, D.; Zhou, Y.; Chou, C.-L.; Wang, X.; Zhao, L.; Zhu, X. Mineralogy and geochemistry of a superhigh-organic-sulfur coal, Yanshan Coalfield, Yunnan, China: Evidence for a volcanic ash component and influence by submarine exhalation. *Chem. Geol.* **2008**, *255*, 182–194. [[CrossRef](#)]
38. China National Standardizing Committee. *Sampling of Coal in Seam*; China National Standardizing Committee: Beijing, China, 2008. (In Chinese)
39. ASTM International. *Test Method for Moisture in the Analysis Sample of Coal and Coke*; ASTM International: West Conshohocken, PA, USA, 2011.
40. ASTM International. *Test Method for Ash in the Analysis Sample of Coal and Coke*; ASTM International: West Conshohocken, PA, USA, 2011.
41. ASTM International. *Test Method for Volatile Matter in the Analysis Sample of Coal and Coke*; ASTM International: West Conshohocken, PA, USA, 2011.
42. ASTM International. *Standard Test for Total Sulfur in the Analysis Sample of Coal and Coke*; ASTM International: West Conshohocken, PA, USA, 2007.
43. ASTM International. *Standard Test Method for Forms of Sulfur in Coal*; ASTM International: West Conshohocken, PA, USA, 2012.
44. Rietveld, H.M. A profile refinement method for nuclear and magnetic structures. *J. Appl. Cryst.* **1969**, *2*, 65–71. [[CrossRef](#)]
45. Taylor, J.C. Computer Programs for Standardless Quantitative Analysis of Minerals Using the Full Powder Diffraction Profile. *Powder Diffr.* **1991**, *6*, 2–9. [[CrossRef](#)]
46. China National Standardizing Committee. *Classification for Quality of Coal. Part 1: Ash*; China National Standardizing Committee: Beijing, China, 2010. (In Chinese)
47. China National Standardizing Committee. *Classification for Quality of Coal. Part 2: Sulfur Content*; China National Standardizing Committee: Beijing, China, 2010. (In Chinese)
48. ASTM International. *Standard Classification of Coals by Rank*; ASTM International: West Conshohocken, PA, USA, 2012.
49. Liu, J.; Song, H.; Dai, S.; Nechaev, V.P.; Graham, I.T.; French, D.; Nechaeva, E.V. Mineralization of REE-Y-Nb-Ta-Zr-Hf in Wuchiapingian coals from the Liupanshui Coalfield, Guizhou, southwestern China: Geochemical evidence for terrigenous input. *Ore Geol. Rev.* **2019**, *115*, 103190. [[CrossRef](#)]

50. Dai, S.; Seredin, V.V.; Ward, C.R.; Hower, J.C.; Xing, Y.; Zhang, W.; Song, W.; Wang, P. Enrichment of U-Se-Mo-Re-V in coals preserved within marine carbonate successions: Geochemical and mineralogical data from the Late Permian Guiding Coalfield, Guizhou, China. *Miner. Depos.* **2015**, *50*, 159–186. [[CrossRef](#)]
51. Ketris, M.P.; Yudovich, Y.E. Estimations of Clarkes for Carbonaceous biolithes: World averages for trace element contents in black shales and coals. *Int. J. Coal Geol.* **2009**, *78*, 135–148. [[CrossRef](#)]
52. Taylor, S.R.; McLennan, S.H. *The Continental Crust: Its Composition and Evolution*; Blackwell: Oxford, UK, 1985.
53. Dai, S.; Hower, J.C.; Finkelman, R.B.; Graham, I.T.; French, D.; Ward, C.R.; Eskenazy, G.; Wei, Q.; Zhao, L. Organic associations of non-mineral elements in coal: A review. *Int. J. Coal Geol.* **2020**, *218*, 103347. [[CrossRef](#)]
54. Finkelman, R.B.; Dai, S.; French, D. The importance of minerals in coal as the hosts of chemical elements: A review. *Int. J. Coal Geol.* **2019**, *212*, 103251. [[CrossRef](#)]
55. Finkelman, R.B. *Modes of Occurrence of Trace Elements in Coal*; U.S. Geological Survey: Reston, VA, USA, 1981.
56. Zhao, C. *Distribution and Enrichment Mechanism of Multi-Metallic Elements Associated with Coal in Ordos Basin. Doctoral Dissertation*; China University of Mining and Technology: Beijing, China, 2015. (In Chinese)
57. Swaine, D.J. *Trace Elements in Coal*; Butterworths: London, UK, 1990.
58. Finkelman, R.B.; Palmer, C.A.; Wang, P. Quantification of the modes of occurrence of 42 elements in coal. *Int. J. Coal Geol.* **2018**, *185*, 138–160. [[CrossRef](#)]
59. Eskenazy, G.M. Rare Earth Elements in a Sampled Coal from the Pirin Deposit, Bulgaria. *Int. J. Coal Geol.* **1987**, *7*, 301–314. [[CrossRef](#)]
60. Arbuzov, S.I.; Chekryzhov, I.Y.; Finkelman, R.B.; Sun, Y.Z.; Zhao, C.L.; Il'enok, S.S.; Blokhin, M.G.; Zarubina, N.V. Comments on the geochemistry of rare-earth elements (La, Ce, Sm, Eu, Tb, Yb, Lu) with examples from coals of north Asia (Siberia, Russian far East, North China, Mongolia, and Kazakhstan). *Int. J. Coal Geol.* **2019**, *206*, 106–120. [[CrossRef](#)]
61. Ren, D.; Zhao, F.; Dai, S.; Zhang, J.; Luo, K. *Geochemistry of Trace Elements in Coal*; Science Press: Beijing, China, 2006.
62. Seredin, V.V.; Finkelman, R.B. Metalliferous coals: A review of the main genetic and geochemical types. *Int. J. Coal Geol.* **2008**, *76*, 253–289. [[CrossRef](#)]
63. Liu, J.; Nechaev, V.P.; Dai, S.; Song, H.; Nechaeva, E.V.; Jiang, Y.; Graham, I.T.; French, D.; Yang, P.; Hower, J.C. Evidence for multiple sources for inorganic components in the Tucheng coal deposit, western Guizhou, China and the lack of critical-elements. *Int. J. Coal Geol.* **2020**, *223*, 103468. [[CrossRef](#)]
64. Hayashi, K.I.; Fujisawa, H.; Holland, H.D.; Ohmoto, H. Geochemistry of ~ 1.9 Ga sedimentary rocks from northeastern Labrador, Canada. *Geochim. Cosmochim. Acta* **1997**, *21*, 4115–4137. [[CrossRef](#)]
65. Dai, S.; Luo, Y.; Seredin, V.V.; Ward, C.R.; Hower, J.C.; Zhao, L.; Liu, S.; Zhao, C.; Tian, H.; Zou, J. Revisiting the late Permian coal from the Huayingshan, Sichuan, southwestern China: Enrichment and occurrence modes of minerals and trace elements. *Int. J. Coal Geol.* **2014**, *122*, 110–128. [[CrossRef](#)]
66. Dai, S.; Zhang, W.; Ward, C.R.; Seredin, V.V.; Hower, J.C.; Li, X.; Song, W.; Wang, X.; Kang, H.; Zheng, L.; et al. Mineralogical and geochemical anomalies of Late Permian coals from the Fusui Coalfield, Guangxi Province, southern China: Influences of terrigenous materials and hydrothermal fluids. *Int. J. Coal Geol.* **2013**, *105*, 60–84. [[CrossRef](#)]
67. Dai, S.; Ren, D.; Chou, C.-L.; Li, S.; Jiang, Y. Mineralogy and geochemistry of the No. 6 Coal (Pennsylvanian) in the Junger Coalfield, Ordos Basin, China. *Int. J. Coal Geol.* **2006**, *66*, 253–270. [[CrossRef](#)]
68. Dai, S.; Ward, C.R.; Graham, I.T.; French, D.; Hower, J.C.; Zhao, L.; Wang, X. Altered volcanic ashes in coal and coal-bearing sequences: A review of their nature and significance. *Earth Sci. Rev.* **2017**, *175*, 44–74. [[CrossRef](#)]
69. Seredin, V.V. A new method for primary evaluation of the outlook for rare earth element ores. *Geol. Ore Depos.* **2010**, *52*, 428–433. [[CrossRef](#)]
70. Dai, S.; Xie, P.; Jia, S.; Ward, C.R.; Hower, J.C.; Yan, X.; French, D. Enrichment of U-Re-V-Cr-Se and rare earth elements in the Late Permian coals of the Moxinpo Coalfield, Chongqing, China: Genetic implications from geochemical and mineralogical data. *Ore Geol. Rev.* **2017**, *80*, 1–17. [[CrossRef](#)]

